

Fault Detection using Parameter Estimation applied to a Winding Machine¹

P. WEBER, S. GENTIL

Laboratoire d'Automatique de Grenoble UMR-CNRS 5528-UJF

E.N.S.I.E.G., BP 46, 38402 Saint Martin d'Hères Cedex - France

Phone: (33) 4 76 82 63 85

Fax: (33) 4 76 82 63 88

weber@lag.ensieg.inpg.fr, gentil@lag.ensieg.inpg.fr

Abstract

On line parameter estimation reflects the process state, but physical parameters are not usually easily estimated in the case of complex systems. This paper presents a sensor or actuator fault detection method based on a classical transfer function parameter estimation algorithm in discrete time domain. Redundant discrete time transfer functions are used to improve the residual generation. The increase of information by redundant equations allows the generation of a signature table. The exploitation of this table, achieved by a distance computation, allows the fault detection and isolation (FDI).

1. Introduction

During the last two decades many fault diagnosis methods based on dynamic models appeared in response to the increasing complexity of process supervision [5]. Such methods are based on:

- state estimation [1] [9],
- parity space [3],
- parameter estimation [6].

On line parameter estimation reflects the process state and therefore might allow fault detection, isolation and identification. In this way the continuous-time estimation technique arouse an increasing research for diagnosis. For processes which are not too complex, the continuous time parameter estimation, makes it possible to come back to physical parameters. We can have a direct knowledge of the different system elements so that the fault identification becomes simplified. Nevertheless, in most cases, it is very difficult to obtain the physical model of the process, because physical parameters are usually not precisely known, particularly for complex systems. Thus, the aim of this work is to test the classical parameter estimation methods (usually found in the control engineer's toolboxes) as a diagnosis tool. In this case,

parameter estimation is followed by a classification technique (based on additional knowledge on the process) in order to achieve the fault identification.

This approach has been applied to the pilot plant represented in figure 1. This process is proposed as an experimental benchmark, so that the results and the methodology can be compared with the other approaches proposed by different members of the IAR diagnosis group.

The system is composed by three DC-motors (M_1 , M_2 , M_3). Their angular velocities are represented by Ω_1 , Ω_2 and Ω_3 , which are respectively controlled by u_1 , u_2 and u_3 . The angular velocity Ω_2 , and the strip tensions T_1 and T_3 between the reels are respectively measured by tachometers and tension-meters. The DC-motors M_1 et M_3 allow the winding or unwinding of the strip but angular velocities Ω_1 , Ω_3 are not measured [4].

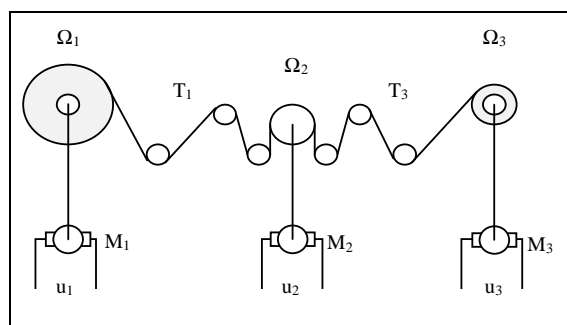


Figure 1: Winding system

This paper is organised as follows: the first section presents the parameter estimation technique that will be used; in the second section, the winding system model is exposed. Afterwards, the redundant transfer function generation which allows the elaboration of the signature table is detailed. The fifth section presents the residual analysis, and an indicator for the fault status of the sensors or actuators is shown. Finally, simulation results are presented before the concluding remarks.

¹ Application on the benchmark winding process for IAR diagnosis group

3. The winding system model

The model can be written as a linear discrete state representation as follows:

$$T_1(k) = a_{T1} \cdot T_1(k-1) + b_{T1v2} \cdot \Omega_2(k-1) + b_{T1v1} \cdot \Omega_1(k-1) \quad (11)$$

$$\Omega_2(k) = a_{v2} \cdot \Omega_2(k-1) + b_{v2T1} \cdot T_1(k-1) + b_{v2T3} \cdot T_3(k-1) + b_{v2u2} \cdot u_2(k-1) \quad (12)$$

$$T_3(k) = a_{T3} \cdot T_3(k-1) + b_{T3v2} \cdot \Omega_2(k-1) + b_{T3v3} \cdot \Omega_3(k-1) \quad (13)$$

$$\Omega_3(k) = a_{v3} \cdot \Omega_3(k-1) + b_{v3T3} \cdot T_3(k-1) + b_{v3u3} \cdot u_3(k-1) \quad (14)$$

$$\Omega_1(k) = a_{v1} \cdot \Omega_1(k-1) + b_{v1T1} \cdot T_1(k-1) + b_{v1u1} \cdot u_1(k-1) \quad (15)$$

The parameters a_{ij} and b_{ij} are not known a priori. The measurements Ω_1 and Ω_3 are not available and thus, in a transfer function representation, putting (15) into (11) and (14) into (13), we can obtain another multivariable model described as follows:

$$A_1(q^{-1}) \cdot T_1(k) = B_{12}(q^{-1}) \cdot \Omega_2(k-d_{12}) + B_{1u1}(q^{-1}) \cdot u_1(k-d_{1u1}) \quad (16)$$

$$A_2(q^{-1}) \cdot \Omega_2(k) = B_{21}(q^{-1}) \cdot T_1(k-d_{21}) + B_{23}(q^{-1}) \cdot T_3(k-d_{23}) + B_{2u2}(q^{-1}) \cdot u_2(k-d_{2u2}) \quad (17)$$

$$A_3(q^{-1}) \cdot T_3(k) = B_{32}(q^{-1}) \cdot \Omega_2(k-d_{32}) + B_{3u3}(q^{-1}) \cdot u_3(k-d_{3u3}) \quad (18)$$

where :

$$A_1(q^{-1}) = 1 - a_{11} \cdot q^{-1} - a_{12} \cdot q^{-2}$$

$$A_2(q^{-1}) = 1 - a_{21} \cdot q^{-1}$$

$$A_3(q^{-1}) = 1 - a_{31} \cdot q^{-1} - a_{32} \cdot q^{-2}$$

$$B_{12}(q^{-1}) = b_{120} - b_{121} \cdot q^{-1}$$

$$\text{et } d_{12} = 1$$

$$B_{1u1}(q^{-1}) = b_{1u10}$$

$$\text{et } d_{1u1} = 2$$

$$B_{21}(q^{-1}) = b_{210}$$

$$\text{et } d_{21} = 1$$

$$B_{23}(q^{-1}) = b_{230}$$

$$\text{et } d_{23} = 1$$

$$B_{2u2}(q^{-1}) = b_{2u20}$$

$$\text{et } d_{2u2} = 1$$

$$B_{32}(q^{-1}) = b_{320} - b_{321} \cdot q^{-1}$$

$$\text{et } d_{32} = 1$$

$$B_{3u3}(q^{-1}) = b_{3u30}$$

$$\text{et } d_{3u3} = 2$$

A first parameter estimation allows to conclude that the gains of the transfer functions relating Ω_2 to T_1 and to T_3 are negligible. The ELS estimator is applied respectively to the following equations, giving the sets of estimates Es_1 , Es_2 and Es_3 :

$$A_1(q^{-1}) \cdot T_1(k) = B_{12}(q^{-1}) \cdot \Omega_2(k-d_{12}) + B_{1u1}(q^{-1}) \cdot u_1(k-d_{1u1}) \quad (19)$$

$$A_2(q^{-1}) \cdot \Omega_2(k) = B_{2u2}(q^{-1}) \cdot u_2(k-d_{2u2}) \quad (20)$$

$$A_3(q^{-1}) \cdot T_3(k) = B_{3u3}(q^{-1}) \cdot u_3(k-d_{3u3}) \quad (21)$$

4. Redundant transfer function generation

In the case of a sensor fault, a bias f_s is added to the measurement of the variable:

$$y(k) = \frac{B(q^{-1})}{A(q^{-1})} \cdot u(k-d) + f_s \quad (22)$$

In the case of an actuator fault, a bias f_a is added to the input u :

$$y(k) = \frac{B(q^{-1})}{A(q^{-1})} \cdot (u(k-d) + f_a) \quad (23)$$

$$y(k) = \frac{B(q^{-1})}{A(q^{-1})} \cdot u(k-d) + \frac{B(q^{-1})}{A(q^{-1})} \cdot f_a$$

After a transient due to the fault :

$$y(k) = \frac{B(q^{-1})}{A(q^{-1})} \cdot u(k-d) + G_s \cdot f_a$$

$$y(k) = \frac{B(q^{-1})}{A(q^{-1})} \cdot u(k-d) + F_a$$

where G_s is the gain of the transfer function.

The estimator that minimises the criterion should reject the perturbations f_s or F_a . Nevertheless, at the moment of the occurrence of a fault, all the estimates are perturbed. Thus, only the transfer functions uncoupled to the faulty measurements or inputs can be estimated without transient perturbation of the parameters.

In a signature table, called diagnostic matrix $D(n,h)$ (Table 1), the set of estimates Es_h perturbed by a bias in the measurements or in the inputs are represented by '1', and the set of estimates not affected are represented by '0'. The signatures represent respectively the faults in T_1 , Ω_2 , T_3 , u_1 , u_2 , and u_3 . Each fault signature is a vector with binary components noted \underline{S}_{gn} , with n varying from 1 to 6 (Table 1).

D	Es_1	Es_2	Es_3
\underline{S}_{g1}	1	0	0
\underline{S}_{g2}	1	1	1
\underline{S}_{g3}	0	0	1
\underline{S}_{g4}	1	0	0
\underline{S}_{g5}	0	1	0
\underline{S}_{g6}	0	0	1

Table 1

As table 1 shows, the signatures \underline{S}_{g1} and \underline{S}_{g4} are identical, as so as \underline{S}_{g3} and \underline{S}_{g6} . It is thus impossible to isolate a fault on T_1 from one on u_1 , as so as for T_3 , and u_3 . This problem is caused by the strong correlation between the measurement and the actuator.

Another fact revealed by the signature table is that the signature of a fault on Ω_2 includes all other signatures. This constitutes a problem for the isolation of simultaneous faults.

The use of additional transfer functions allows to extend the signature table. This extension is aimed at discrimination between very similar signatures, by adding new symptoms [7]. It can be done by putting eq. (20) into (19) to obtain a model that relies T_1 to u_1 and u_2 : thus we can exhibit a uncoupling between T_1 et Ω_2 .

The parameters estimated in this way will not be sensitive to the perturbation on Ω_2 . The same procedure can be applied for (21) and (20) and so, the sets of estimates Es_4 and Es_5 can be obtained from:

$$A_{11}(q^{-1}).T_1(k)= \quad (24)$$

$$B_{11u2}(q^{-1}).u_2(k-d_{11u2})+ B_{11u1}(q^{-1}).u_1(k-d_{1u1})$$

$$A_{33}(q^{-1}).T_3(k)= \quad (25)$$

$$B_{33u2}(q^{-1}).u_2(k-d_{33u2})+ B_{33u3}(q^{-1}).u_3(k-d_{3u3})$$

where:

$$\begin{aligned} A_{11}(q^{-1}) &= 1 - a_{111} \cdot q^{-1} - a_{112} \cdot q^{-2} - a_{113} \cdot q^{-3} \\ A_{33}(q^{-1}) &= 1 - a_{331} \cdot q^{-1} - a_{332} \cdot q^{-2} - a_{333} \cdot q^{-3} \\ B_{11u2}(q^{-1}) &= b_{11u20} - b_{11u21} \cdot q^{-1} & \text{et } d_{11u2} &= 2 \\ B_{11u1}(q^{-1}) &= b_{11u10} - b_{11u11} \cdot q^{-1} & \text{et } d_{1u1} &= 2 \\ B_{33u2}(q^{-1}) &= b_{33u20} - b_{33u21} \cdot q^{-1} & \text{et } d_{33u2} &= 2 \\ B_{33u3}(q^{-1}) &= b_{33u30} - b_{33u31} \cdot q^{-1} & \text{et } d_{3u3} &= 2 \end{aligned}$$

The signature table $D(n,h)$, is represented in table 2.

D	Es ₁	Es ₂	Es ₃	Es ₄	Es ₅
<u>S_{g1}</u>	1	0	0	1	0
<u>S_{g2}</u>	1	1	1	0	0
<u>S_{g3}</u>	0	0	1	0	1
<u>S_{g4}</u>	1	0	0	1	0
<u>S_{g5}</u>	0	1	0	1	1
<u>S_{g6}</u>	0	0	1	0	1

Table 2

The problem of signatures S_{g1} and S_{g4} which are the same (as for S_{g3} S_{g6}) is not solved, but the signature S_{g2} doesn't include the others, and allows a better discrimination.

5. Residual analysis and fault indicator

The on-line parameter estimation with a long horizon estimator allows to follow the slow variations of the parameters. This kind of variations are not considered as faults, but caused by the ageing of the process. A second estimator based on a short horizon, allows to follow fast variations considered as a symptom of the fault. The long horizon parameters are estimated by on-line ELS algorithm with a forgetting factor equal to 1; and the short horizon estimator is computed with a smaller forgetting factor (0.99 in the following).

The residual generation for diagnosis is computed for each parameter by the difference between the long horizon estimates Θ_j and the short horizon estimates θ_j (26).

$$r_j^h = \Theta_j^h - \theta_j^h \quad (26)$$

where h is the index corresponding to the set of estimates Es_h .

The comparison of r_j^h with an adapted threshold which depends on the estimate variance allows to detect a significant variation of the estimation.

The result of this evaluation composes the vector S^h . The components s_j^h of the vector S^h are binary: 1 if the threshold is bypassed, and 0 otherwise.

A degree u_h of estimation variations can be computed for the set of estimates Es_h (27):

$$u_h = \frac{1}{p^h} \sum_{j=1}^{p^h} s_j^h \quad (27)$$

where p^h represents the number of estimated parameters of the set of estimates Es_h . The set of symptoms u_h constitutes the vector U .

The decision method is achieved comparing U with the different signatures S_{gn} in table 2.

The decision function noted $F_E(\underline{S}_{gn})$ represents the confidence on the sensors or the actuators and takes the following values:

$$F_E(\underline{S}_{gn}) = 0 \quad \text{no fault,}$$

$$F_E(\underline{S}_{gn}) \in]0,1[\quad \text{suspicion of fault,}$$

$$F_E(\underline{S}_{gn}) = 1 \quad \text{fault.}$$

The Hamming's distance formula (28) is used to generate the fault indicator $F_E(\underline{S}_{gn})$ [10].

$$\Delta(U, \underline{S}_{gn}) = \frac{1}{H} \sum_{h=1}^H |u_h - D(n, h)| \quad (28)$$

with H the number of the sets of estimates Es_h

The fault indicator $F_E(\underline{S}_{gn})$ is given by the similarity between the signatures and the symptom vector U :

$$F_E(\underline{S}_{gn}) = 1 - \Delta(U, \underline{S}_{gn}) \quad (29)$$

In the case of simultaneous failures on different sensors or actuators, the Hamming distance (28) is modified as follows:

$$\Delta_M(U, \underline{S}_{gn}) = \frac{1}{W_n} \sum_{h=1}^H \{ |u_h - D(n, h)| \cdot D(n, h) \} \quad (30)$$

where W_n is the number of elements of $D(n,h) \neq 0$.

The fault indicator $F_E(\underline{S}_{gn})$ (29) is computed as:

$$F_E(\underline{S}_{gn}) = 1 - \frac{1}{W_n} \sum_{h=1}^H \{ |u_h - D(n, h)| \cdot D(n, h) \} \quad (31)$$

6. Application

The analysis of the method above described was done with a simulator of the system. The inputs u_1 u_2 and u_3 are

step signals at times 50, 100 and 150 (the sampling period is 0.1s). The signal to noise ratio was fixed to 31 dB. The fault was simulated as a bias of 10 % of the steady state value on the sensor Ω_2 , and appears at time 300 (Figure 2).

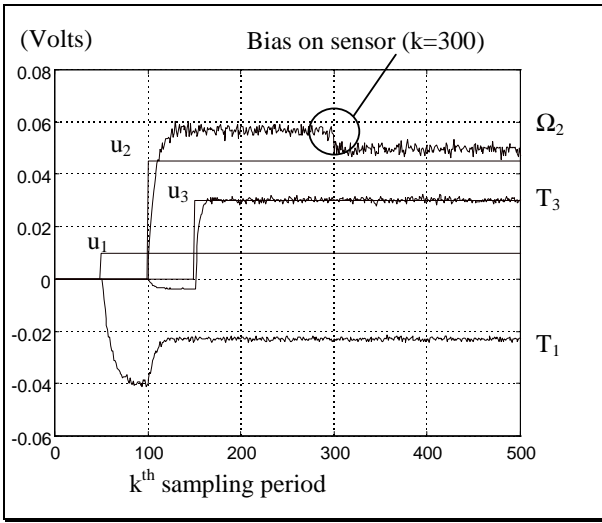


Figure 2 : Variation of the inputs and of the measurements around the operating point

Figures 3 and 4 present the evolution of the short horizon parameter estimations. The estimates of c_i are not represented due to their high sensitivity to the noise and their slower convergence. The decision is done only from a_i and b_i estimates. Moreover, the estimates a_{113} and b_{33u21} are very close to zero and thus, they are not taken into account by the set of estimates Es_4 and Es_5 .

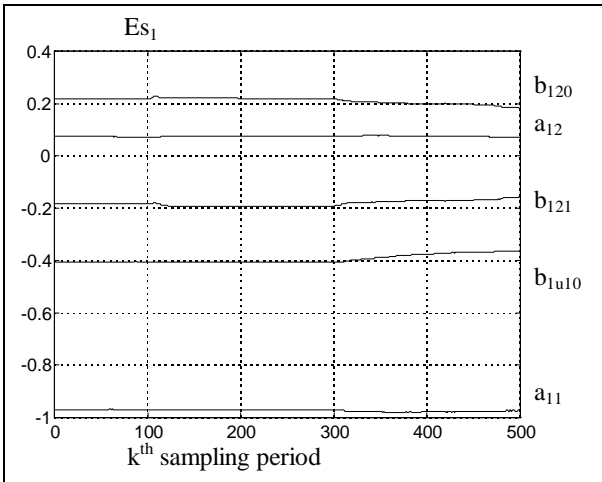


Figure 3 : Evolution of the set of estimates Es_1 .

Figure 3 shows the evolution of the set of estimates Es_1 . A variation of b_{1u10} can be seen (with a small delay

$k=305$) while b_{120} and b_{121} are perturbed since the fault apparition (301). The variations of the estimate a_{11} are shown in figure 4. The variance of the estimate is $0.5 \cdot 10^{-4}$ at time $k=300$.

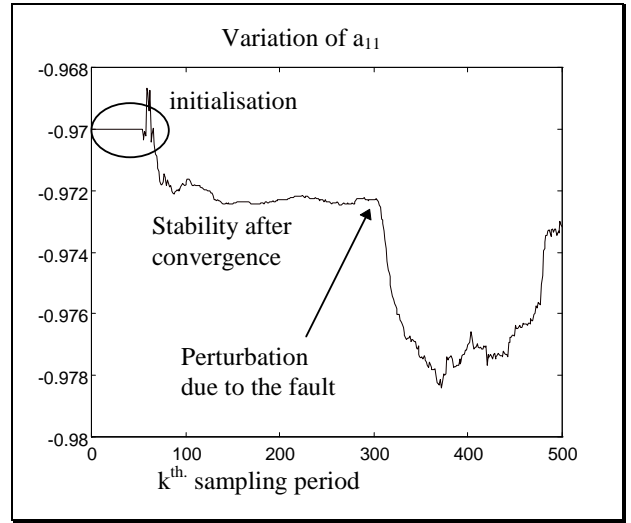


Figure 4 : Evolution of Es_1 estimate a_{11}

Figure 5 shows the Es_4 short horizon estimates. They are not perturbed by the fault on Ω_2 as expected by table 2.

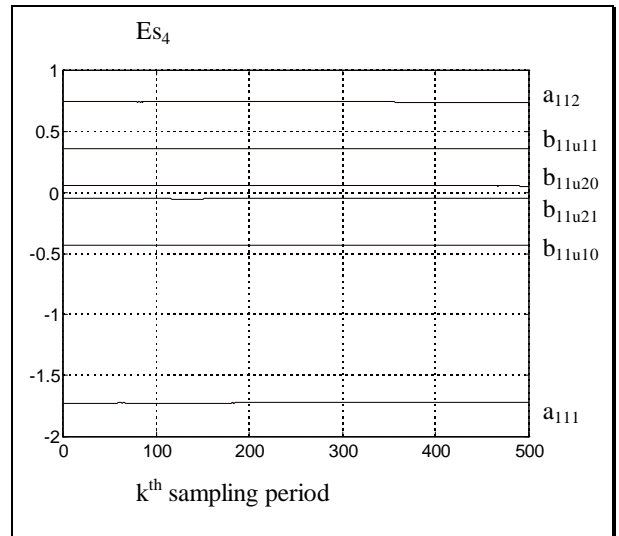


Figure 5 : Evolution of the set of estimates Es_4 .

Figures 6 and 7 show the evolution of the fault indicator $F_E(\underline{S}_{gn})$.

Figure 6 represents the decision taken from Es_1 , Es_2 and Es_3 (Table 1). In this case, it is impossible to isolate the fault because after $k=300$ the indicators report faults in T_1 , Ω_2 , u_1 and u_2 .

Figure 7 represents the decision relying on all the sets of estimates, taking into account the transfer function redundancy which has allowed to generate table 2. The isolation is correct, the indicator $F_E(S_{g2})$ corresponding to a fault on Ω_2 is greater than zero from time 303 (delay of 3 sampling periods), and is always greater than the other indicators.

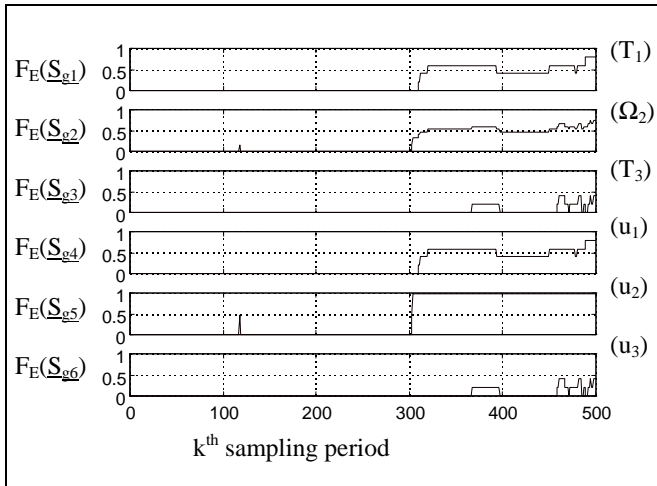


Figure 6 : Evolution of the fault indicators (Table 1)

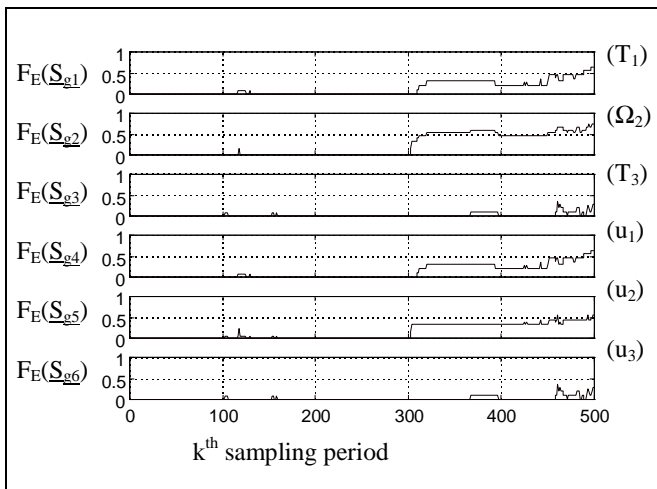


Figure 7 : Evolution of the fault indicators (Table 2)

7. Conclusion

This paper proposes a method for detection and isolation of a bias on sensors or actuators. The use of the estimation redundancy has allowed the generation of a decision procedure for fault isolation. Nevertheless some limitations of the redundancy of transfer functions, due to the system structure, are underlined.

The future work will be focused on:

- The use of fuzzy logic for the residual evaluation in order to process more information, in particular the quality of the residual evaluation, qualified by the *frankness* or *persistence* of parameter deviations.
- The use of fuzzy logic in the decision making method.
- The management of the estimation deviations due to noise in the case of non-persistent excitation.
- The introduction of the direct estimation of a mean value change in the error.
- The test of this method on the real process.

References

- [1] Alcorta Gracia E., Frank P.M. : Deterministic non-linear observer-based approaches to fault diagnosis : a survey. Control Eng. Practice, Vol. 5, No. 5, pp. 663-670, 1997.
- [2] Barraud A., Roche-Zamboni I. : Identification multivariable en ligne : Une approche paramétrique et structurale simultanée. APII, Vol. 22, No. 2, pp. 177-199, 1988.
- [3] Gertler J. : Fault detection and isolation using parity relations. Control Eng. Practice, Vol. 5, No. 5, pp. 653-661, 1997.
- [4] Hittinger J.-M. : Identification, commande et diagnostic d'un système multivariable d'entraînement de bande. Rapport de diplôme d'ingénieur CNAM note interne CRAN, 1996.
- [5] Isermann R., Ballé P. : Trends in the application of model-based fault detection and diagnosis of technical processes. Control Eng. Practice, Vol. 5, No. 5, pp. 709-719, 1997.
- [6] Isermann R. : Fault diagnosis of machines via parameter estimation and knowledge processing - Tutorial paper. Automatica, Vol. 29, No. 4, pp. 815-835, 1993.
- [7] Koscielny J.M., Bartys M.Z. : Smart positioner with fuzzy based fault diagnosis. IFAC, SAFEPROCESS'97, Vol. 2, pp. 603-608, Kingston Upon Hull, UK, Aug. 26-28, 1997.
- [8] Ljung L. : System identification : Theory for the user. Prentice-Hall Englewood Cliffs, New Jersey, 1987.
- [9] Patton R.J., Chen J. : Observer-based fault detection and isolation : robustness and application. Control Eng. Practice, Vol. 5, No. 5, pp. 671-682, 1997.
- [10] Theilliol D., Weber P., Ghetie M., Noura H. : A hierarchical fault diagnosis method using a decision support system applied to a chemical plant. IEEE International Conference on Systems, Man, & Cybernetics, Oct 22, Vancouver - Canada, 1995.